INTERNATIONAL JOURNAL OF CLIMATOLOGY
Int. J. Climatol. (2016)
Published online in Wiley Online Library
(wileyonlinelibrary.com) DOI: 10.1002/joc.4895

RMetS
Royal Meteorological Society

Temperature extremes in the Argentina central region and their monthly relationship with the mean circulation and ENSO phases

Matilde Rusticucci,[a,b]* Mariana Barrucand[a,b] and Soledad Collazo[a,b]

[a] *Departamento de Ciencias de la Atmósfera y los Océanos, Facultad de Ciencias Exactas y Naturales, Universidad de Buenos Aires (DCAO-FCEN-UBA), Argentina*

[b] *Consejo Nacional de Investigaciones Científicas y Técnicas (CONICET), Buenos Aires, Argentina*

ABSTRACT: The aim of this study is to analyse the interannual variability of monthly climatic indices of extreme daily temperature in the central-north region of Argentina throughout a year and its relationship with the atmospheric circulation. The impact of El Niño-Southern Oscillation (ENSO) over different temperature indices throughout the year is specially analysed. Globally used indices in the 1970–2010 period are utilized for this purpose. The trends of temperature extremes show warming conditions in several months, especially in October and November. In order to find possible forcings of extreme temperature in the region at monthly scale, the co-variability with other circulation monthly time series such as changes in the intensity of Southern Hemisphere semi-permanent anticyclones and the intensity of the subtropical jet were studied. The main finding was a systematic shift of the South Atlantic anticyclone towards the west over the decades in June and August, which might hinder the cold advections over the region surveyed. Moreover, the influence of the variation on the intensity of the subtropical jet over extreme events showed significant positive (negative) correlations between the intensity of the jet and the frequency of cold (warm) indices in a great number of months. Finally, the influence of the ENSO phases on each of the temperature extremes analysed was studied. It was found that under El Niño conditions, minimum temperatures are affected quite evenly throughout the year, fostering the occurrence of warm nights. The impact of the El Niño event on the maximum extreme temperatures, however, shows seasonal differences. Between July and September warm days conditions are fostered, while between November and February the opposite (cold days) can be seen. This results in a decrease in the temperature range in the region surveyed during the summer months under El Niño conditions.

KEY WORDS monthly extreme temperature events; trends; interannual variability ENSO; South Atlantic anticyclone; subtropical jet stream; Argentina

Received 3 November 2015; Revised 15 June 2016; Accepted 19 June 2016

1. Introduction

Society is affected by extreme meteorological and climate phenomena. Nature and the gravity of its impacts do not only depend on their intensity, but also on the exposition and vulnerability of the society affected by them. Since its Third Assessment Report (Houghton *et al.*, 2001), the Intergovernmental Panel on Climate Change (IPCC) indicates that the impact generated by climate change will be particularly noticeable by extreme events. These changes are of the utmost importance since they may cause tension or exceed our present adaptations to climate variability. According to the IPCC (2012) Special Report on Managing the Risks of Extreme Events and Disasters to Advance Climate Change Adaptation (SREX), this problem is influenced by a wide range of factors, including the anthropogenic climate change, natural climate variability and socio-economic development. Climate change and variability on several scales alter the frequency, intensity, spatial extension and duration of extreme meteorological and climate events and, therefore, their impact as well.

In order to study temperature extreme events, the first step is to have trustworthy and plentiful data series, with few missing data, which will make it possible to establish if there is an actual climate change and/or variability. In Argentina, Rusticucci and Barrucand (2001) studied the variability of mean values, standard variations and asymmetries of maximum and minimum summer and winter temperatures for a great number of weather stations located across the country. First, the quality of the data was verified since they had not been previously used in climate studies of this type.

Then, Barrucand and Rusticucci (2001) studied the variability of the frequency of daily extreme warm and cold events in both summer and winter. Part of this information was used in a continental-scale study (Vincent *et al.*, 2005), where trends of some indices of extreme temperatures in South America to the south of the Equator are

* Correspondence to: M. Rusticucci, Departamento de Ciencias de la Atmósfera y los Océanos, Facultad de Ciencias Exactas y Naturales, Universidad de Buenos Aires, Intendente Güiraldes 2160, Ciudad Universitaria Pab II, 1428 Buenos Aires, Argentina. E-mail: mati@at.fcen.uba.ar

presented. This study did not find consistent changes in the indices based on the maximum temperature on the continent, although there were changes in the indices based on the minimum temperature with increases in the percentage of warm nights and decrease in the percentage of cold nights in the 1960–2000 period. Subsequently, Skansi *et al.* (2013) further spread the network of weather stations analysed across the South American region, showing that the trends at an annual scale for the 1969–2009 period provided evidence of warming and wetting across the region.

When applying the theory of extreme values to temperatures, Tencer and Rusticucci (2012) showed that there is a decrease in the intensity of extreme warm events as well as an increase in the frequency of their occurrence in the second half of the past century. A review of several studies on the variability of temperature extremes in South America can be seen in Rusticucci (2012), where it is highlighted that several of these studies agree in that the most significant trends occur in the minimum temperature indices, with positive trends in the occurrence of warm nights and negative trends in cold nights.

At seasonal scale, Rusticucci and Barrucand (2004) analysed the trends in the mean, standard deviation, and maximum and minimum extreme temperatures in summer and winter, finding values of negative trends in the number of cold nights and warm days in summer, while in winter, no defined pattern was observed. Subsequently, Barrucand (2008) showed that in winter it is possible to observe a marked intermonthly variability in the central region of the country, because the signs of the trends are reversed in July and August in the 1959–2003 period analysed. Therefore, it is necessary to study the possible causes of intermonthly variability of the trends in temperature extremes in the central region of Argentina, based on the analysis of decadal and interannual changes in large-scale atmospheric circulation.

Argentina spans a wide range of latitudes, extending from the circumpolar high latitude zone of westerly winds in the south, through a transition zone, to the subtropical zone of mainly easterly winds in the north (Gosling *et al.*, 2011). The Andes are the most important mountain range in the Southern Hemisphere. Consistent with their impressive length, continuity and height, the Andes significantly disrupt the atmospheric circulation, resulting in a variety of mesoscale and synoptic phenomena, as well as sharply contrasting climate conditions along the eastern and western slopes and adjacent lowlands (Garreaud, 2009). Figure 1 presents a scheme of the low-level atmospheric flow and the major climate features of South America (adapted from Garreaud, 2009).

The South Atlantic anticyclone dominates the low-level circulation east of the Andes. It reaches greater intensity in winter than in summer (Prohaska, 1976). The easterly flow from the equatorial Atlantic Ocean turns south towards the subtropical region when reaching the proximity of the Andes, resulting in a predominant meridional component from the north all year long.

Inside the continent, over the slope extending from Chaco to Los Andes mountain range, a summer

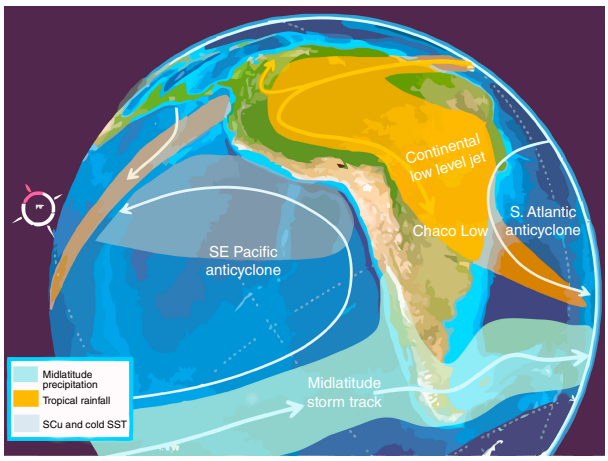

Figure 1. Main surface circulation features over South America (adapted from Garreaud, 2009).

low-pressure system can be observed: the Chaco Low. Owing to its thermal nature, its development rarely involves levels >700 hPa. Towards the SW of its core, another system develops: the Argentine Northwest Low. It is an intermittent system of thermal-orographic nature that seems to be an appendix of the Chaco Low. Its intensity is higher during summer. A detailed description of these systems can be found in Seluchi and Saulo (2012).

The continental low over the Chaco region drives northerly flow that usually features a low-level jet (LLJ) structure with its core at about 1 km a.g.l. and about 200 km east of the Andean foothills (Saulo *et al.*, 2000; Marengo *et al.*, 2004). The northerly LLJ transports vast amounts of water vapour from the Amazon Basin into the subtropical plains of the continent (Garreaud, 2009)

South of 40°S, low-level westerly flow prevails year round over the adjacent oceans and the continent. The region is populated by migratory surface cyclones and anticyclones, an integral part of the baroclinic eddies. Synoptic-scale baroclinic eddies migrating along mid-latitude storm tracks not only influence daily weather but also play a crucial role in the climate system by systematically transporting heat, moisture and angular momentum (Nakamura *et al.*, 2004). The mid-latitude westerlies extend through the entire troposphere, reaching a maximum speed (the jet stream) in the upper troposphere (Garreaud *et al.*, 2009).

Northward intrusions of cold fronts are responsible for the cooling condition at the studied region, north to 40°S, and therefore warming in this region predominates when the frontal zone remains at higher latitudes. Indeed, the northward displacement of the fronts is associated with a similar shift of the subtropical jet, producing the strengthening of the flow in the northern edge of the westerly belt and its weakening in mid-latitudes (Barros *et al.*, 2002). The opposite occurs when the frontal zone remains within middle latitudes. Stronger subtropical upper level flows are accompanied with more frequent and northward intrusions of cold fronts. This is associated with lower temperatures over central Argentina.

Several studies have extensively documented that El Niño-Southern Oscillation (ENSO) explains a large part of the interannual variability of the Southern Hemisphere (Vera *et al*., 2004). The atmospheric circulation response to ENSO events over the Southern Hemisphere basically consists of an equivalent-barotropic wavetrain that extends southeastward from the central tropical Pacific and it turns equatorward reaching South America (Karoly, 1989). This wavetrain has been identified as the Pacific–South American pattern and is associated with the second and third leading patterns of the circulation anomaly interannual variability in the Southern Hemisphere (Mo, 2000).

During El Niño years, over South America, it is possible to observe a cyclonic anomaly located at the southern tip of the continent and an anticyclonic anomaly off the eastern coast, both fostering an enhanced precipitation over southeastern South America (SESA), as described by Grimm *et al.* (2000). It also shows that the impact on rainfall in summer is much weaker than in spring. In terms of mean surface temperature, Barros *et al.* (2002) found positive anomalies in El Niño phase between 1963 and 1990 only during the austral winter in the SESA region. Opposite patterns of temperature and precipitation anomalies are observed during La Niña in South America.

Among the research conducted to study the influence of this phenomenon on the frequency of extreme temperatures in the country, the work by Rusticucci and Vargas (2002) can be mentioned. These authors found that different episodes of La Niña compared to Neutral give rise to more homogeneous effects on the spells of temperature extremes than do the El Niño phases, especially in the case of cold events. More recently, Agosta and Barrucand (2012) describe the modulation of the ENSO positive phase on the frequency of warm nights over subtropical Argentina in the winter months (JJA), finding a positive association between the high frequency of warm nights and the anomalous warming of the central equatorial Pacific for the 1979–2008 period.

Kenyon and Hegerl (2008) analysed the influence of large-scale modes of climate variability on worldwide summer and winter temperature extremes. In particular, over the region studied, they found that under El Niño conditions, significantly more warm extremes were observed, mainly minimum temperature extremes during the extended cold season (May–October).

Arblaster and Alexander (2012) examined the impact of the ENSO on temperature extremes using HadEX2, the observed gridded data set of climate extremes indices. They showed warmer DJF composites of maximum monthly daily maximum temperatures for warm ENSO events over central Argentina.

Considering that previous studies on temperature extremes focused on relative short periods and/or on annual or seasonal scales, this study enabled further progress on the analysis of monthly extreme temperature indices in Argentina, giving special consideration to the central region, the most populated and economically relevant. A greater number of stations were incorporated in the region compared to previous studies and the period analysed was extended to more recent years.

First, a trend analysis of monthly climatic indices of extreme temperatures in central Argentina was performed in order to analyse the interannual variability of such indices throughout the year. Then, the co-variability with some time series related with the atmospheric circulation (such as the intensity of semi-permanent anticyclones, the LLJ and the subtropical jet) were evaluated in order to obtain information of possible forcings of extreme temperature in the region at monthly scale. Special attention was given to the changes occurred on both warm and cold extremes at different ENSO phases.

Section 2 accounts for the data and methodologies used. Section 3 shows the trends in indices and analyses decadal changes in the position of both anticyclones and the subtropical jet stream, and identifies its correlation with the indices of temperature extremes. There is also an analysis on the influence of ENSO on the probability of occurrence of said extremes. Lastly, a summary and conclusions is presented in Section 4.

2. Data and methodology

Daily minimum and maximum temperatures were used, which were taken from 33 conventional weather stations located north of 40°S in Argentina. These data were provided by the National Institute of Agricultural Technology (INTA) on its website (http://siga2.inta.gov.ar/en/datoshistoricos/ consulted in June 2013), of which 21 were retained since they had <10% of missing data in the 1970–2010 period (Figure 2). Subsequently, 15 stations of the National Meteorological Service (SMN) were incorporated in the central region of the country in order to get a more comprehensive outlook on the behaviour shown by temperature extremes in this Argentina region, which exhibited the greatest intermonthly variability (Barrucand, 2008).

The freely available R-Climdex software was used (at: http://etccdi.pacificclimate.org/software.shtml) in order to perform a quality control check of each station. In all cases, it was verified that the maximum temperature had to be higher than the minimum temperature. Data with values far above or below the expected values were also checked. These were analysed individually, considering the information from nearby stations and temperature evolution on previous and subsequent days.

After analysing the outliers, four extreme temperature indices were calculated on a monthly basis, following the guidelines established by international literature on the subject based on recommendations by the WMO Joint Commission for Climatology (CCl)/CLIVAR/JCOMM Expert Team on Climate Change Detection and Indices (ETCCDI): cold nights (TN10), percentage of days with minimum temperature below the 10 percentile; warm nights (TN90), percentage of days with minimum temperature above the 90 percentile; cold days (TX10), percentage of days with maximum temperature below

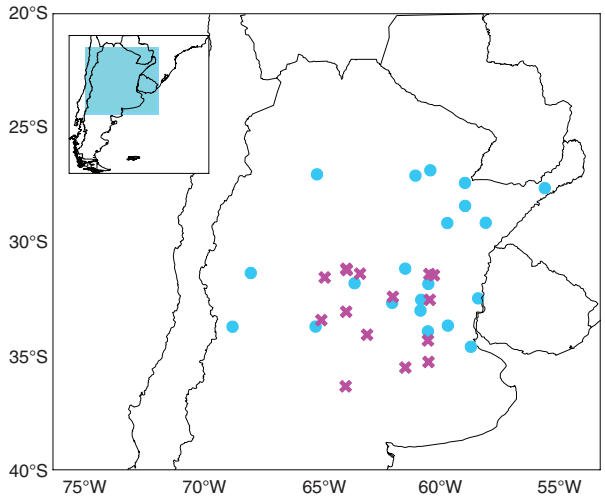

Figure 2. INTA stations used with <10% of missing data (circles) and SMN stations (crosses) of the central region of the country.

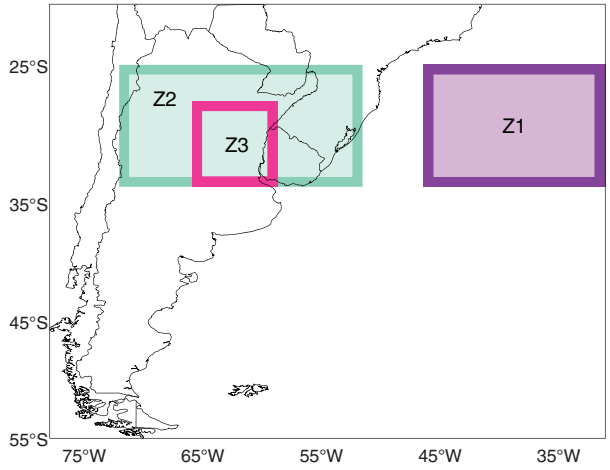

Figure 3. Regions on which the different variables were spatially averaged: Z1 (monthly mean anomalies of geopotential height at 1000 hPa); Z2 (monthly mean zonal wind at 250 hPa); Z3 (monthly mean meridional wind at 925 hPa).

the 10 percentile and warm days (TX90), percentage of days with maximum temperature above the 90 percentile. Considering the data available in different periods, the percentiles used to construct the indices were calculated with the 1981–2010 base period. The ETCCDI has a mandate to address the need for the objective measurement and characterization of climate variability and change by providing international coordination and helping organizing collaboration on climate change detection and indices relevant to climate change detection, and by encouraging the comparison of modelled data and observations.

As to the statistical distribution of indices of temperature extremes, Barrucand (2008) shows that although series do not have a strictly normal distribution, for a significant level of 10%, due to their characteristics, the distribution is not 'too far' from a normal one, such as its condition of unimodal distribution and the mean that is close to the median, among other aspects. Linear trends were calculated for the 1970–2010 period. Then, these trends were statistically tested with the hypothesis test for the slopes (β), which assumes normality, with a significance of 5 and 10% (Hoel, 1971). Trends were also tested by using the Kendall-tau nonparametric test (Sen, 1968), following the methodology used in many previous studies on extreme indices (Vincent *et al*., 2005; Alexander *et al*., 2006; and Haylock *et al*., 2006, among others), with which it was possible to obtain similar results to the ones previously achieved.

In order to analyse the relationship between the indices of temperature extremes and mean circulation, some atmospheric variables were studied: sea level pressure, 1000 hPa geopotential height, 925 hPa meridional wind and zonal wind at 250 hPa. Trying to assure more robust results, different data sets were used. NCEP/NCAR R1, NCEP/DOE AMIP II R2, 20CRv2c, ERA-Interim and JRA-55 reanalysis were considered for this purpose. Results showed similar values in almost all calculi, except 20 CRv2c, which present some differences, but do not yield opposing results. Considering the data sets with congruent results, the NCEP1 (http://www.esrl.noaa.gov/psd/cgi-bin/data/composites/printpage.pl, consulted in June 2014) is used (Supporting information Figures S1–S17 is provided with some results obtained with other data sets).

In order to estimate the interannual variability between the indices of temperature extremes and the intensity of the semi-permanent South Atlantic anticyclone (AI), the Spearman's correlation coefficient (Wilks, 2006) was calculated between both variables and its significance was tested (Freund *et al.*, 2000). Considering the region with the maximum variability of the South Atlantic anticyclone, the time series of monthly mean geopotential height anomalies at 1000 hPa (G1000) in the 1971–2010 period were analysed. For this purpose, a spatial average of G1000 was calculated for the Z1 region located between 25°–35°S and 30°–45°W (Figure 3).

Before correlations were calculated, linear trends were filtered from the monthly series since in non-stationary series the correlation might be due precisely to trend patterns, which could give rise to spurious correlations between series (Arnau Gras, 2001). For that purpose, the regression straight line adjusted by minimal squares was deduced from the observations both for the extreme temperature indices and for G1000 in Z1 region.

An analogous procedure was followed with the monthly mean zonal wind at 250 hPa spatially averaged in the Z2 region, located between 25°–35°S and 50°–70°W (Figure 3). This region was selected to represent the subtropical jet, which is located approximately at 25°S in winter and 35°S in summer (Barros *et al.*, 2002).

Finally, in order to assess whether there are differences in the occurrence frequency of extreme events between El Niño phase and climatology, monthly frequency distributions were performed by comparing them. The same analysis was made for La Niña. To carry out the frequency distributions, data were considered jointly for all stations in the central region of the country. In this manner, for each

month of the year, frequency distributions for the entire region were calculated for each ENSO phase and for each of the four extreme indices. Monthly climatology distributions were obtained by using all data sets in the region without classifying them into ENSO phases.

The extreme indices classification according to ENSO events was carried out considering the Oceanic Niño Index (ONI) obtained from the National Oceanic and Atmospheric Administration (NOAA) website. The ONI index is based on the sea surface temperature anomalies in the Niño 3.4 region (5°N–5°S, 120°–170°W), identified by the acronym ERSST v.4, taking the 1981–2010 period as a base period. According to the historical standards, to be classified as an El Niño or La Niña event, the ±0.5 °C thresholds must be surpassed at least for 5 consecutive months when the 3-month running mean of ERSST.v4 is conducted. This being a 3-month index, its value was assigned to the intermediate month of the period, and the ENSO events in the 1971–2010 period surveyed were taken into account. It was chosen because it is the standard index that NOAA uses for identifying El Niño and La Niña events in the tropical Pacific.

The nonparametric Wilcoxon rank sum (Wilcoxon, 1945) was used to test the differences between frequency distributions, considering as null hypothesis that the distribution of the temperature extremes during El Niño (or La Niña) phase is no different from that of climatology. The Wilcoxon rank-sum test is equivalent to the Mann–Whitney U-test. The Mann–Whitney U-test is a nonparametric test for equality of population medians of two independent samples X and Y. The Mann–Whitney U-test statistic, U, is the number of times y precedes an x in an ordered arrangement of the elements in the two independent samples X and Y. It is related to the Wilcoxon rank-sum statistic (W) by the following expression:

$$U = W - \frac{n_X\left(n_X + 1\right)}{2} \tag{1}$$

where n_X is the size of the sample X. Ec.1 shows that the Mann–Whitney U statistic is a linear function of the Wilcoxon rank-sum test statistic. Thus, all the properties of the two tests are the same. A confidence-interval procedure based on the Wilcoxon rank-sum test leads to the same results as the one based on the Mann–Whitney test (Gibbons and Chakraborti, 2011). If the Wilcoxon rank-sum statistic obtained by performing the test was minor or equal to the significance level, established in 0.05, the null hypothesis was rejected.

3. Results and discussions

3.1. Trends in temperature extremes in the 1970–2010 period

For each of the four indices of extreme temperature and for each month of the year, linear trends were calculated and tested at a significance of 5 and 10% for the period 1970–2010. In general, significant trend values at 5% vary between 9.8 and 21.3% of days with extreme temperature in the 41-year period analysed (Figure 4).

The monthly detail shows that, with respect to the cold nights (TN10), the months of October and November stand out with significant negative trends in >50% of stations. This reflects a decrease in the occurrence of TN10 during the period analysed. In general, it is possible to observe negative trends in spring and early summer (from October through January) and also in March and June; and no significant trends in winter.

The major changes in the frequency of warm nights, TN90, can be observed in November, with a large number of stations exhibiting significant positive trends (>60%). Table 1 shows the percentage of stations by month with significant trends and their corresponding signs. In addition to what was previously observed for TN10, this result makes it possible to infer that during said month, the greatest increase in the minimum extreme temperature was detected. Something similar, although not as marked, occurs in October, when it is possible to see a decrease in the number of cold nights over time. It is also possible to view that from August to November positive trends – not significant, though – prevail, as is also the case in March.

In regard to cold days, TX10, there are no significant changes except in the case of more limited regions in the central-east of the country. Nevertheless, March, June and October present significant negative trends as in TN10. These months show the major decrease of cold nights and days.

The frequency of warm days, TX90, shows that positive trends prevail throughout the year, especially in August and November. December appears to behave differently, with significant negative trends in the central-south region. In August, stations with significant trends at 5% are mostly spread along the eastern side of the region studied, while in November they are located further south and central. If results obtained for TX10 and TX90 are considered jointly, it is possible to see an increase in the maximum temperature in October, November (mainly due to the increase in the number of warm days) and March (especially due to the decrease in cold days).

In general, cold extremes show a decreased occurrence both for minimum and maximum temperatures while warm extremes show an increased occurrence (especially the frequency of warm days between August and November). These trends foster warmer conditions in the region.

Owing to the fact that previous studies (Rusticucci and Barrucand, 2004; Vincent *et al*., 2005; Skansi *et al*., 2013) used different periods to calculate the trend and conducted an annual or seasonal study of those trends, it is difficult to compare results because the trend is strongly dependent on the period over which it is calculated. However, it was possible to see a decrease in the occurrence of cold extremes (mainly in the minimum temperature) and an increase of warm extremes in the region studied, which turns out to be consistent with the findings from the studies previously mentioned and by Hartmann *et al.* (2013) in the IPCC AR5.

Unlike the results found by Barrucand (2008), a marked reversion of trend signs was not observed between July and August. This discrepancy could be due to the different

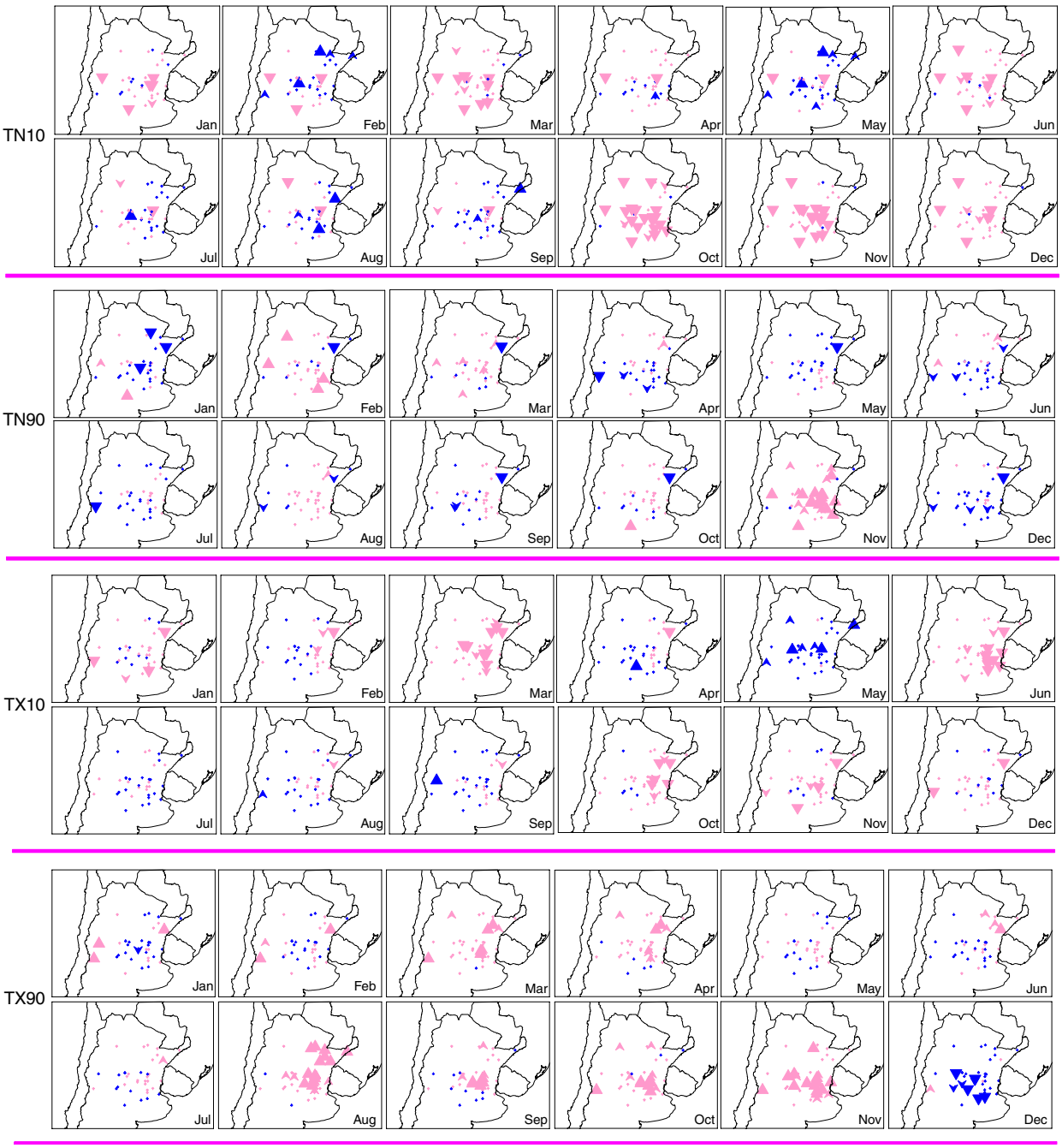

Figure 4. Spatial distribution of trends for TN10, TN90, TX10 and TX90; where downward (upward) facing triangles indicate negative (positive) trends. The smallest triangles are not significant, those who follow in size (▲) are significant at 10% and the biggest are significant at 5% (▲). Downward (upward) facing triangles at indices TN10 and TX10 indicate warming (cooling) condition and vice versa with TN90 and TX90.

periods used to calculate the trend and, to a lower extent, to the different base periods used to calculate the indices.

In the case of the INTA weather stations that had longer series, a sensitivity analysis on the trend was conducted with two types of computations:

i. Considering extreme indices calculated with percentiles obtained with different base periods
ii. Considering extreme indices calculated with percentiles obtained with the same base period, but then computing the trend over different periods (complete period of data 1959–2010 and 1970–2010 period)

Results showed that the second factor was more important than the first, i.e. the period over which the trend of extreme indices is calculated affects the trend more than the base period used to calculate the indices.

3.2. Signals in atmospheric circulation

3.2.1. Changes of the mean intensity of semi-permanent anticyclones

The increase (reduction) of the zonal geopotential gradient between the South Atlantic anticyclone and the Chaco Low, representative of the north component of the

Table 1. Percentage of stations with significant trends, and their respective signs, for each month and for each extreme index. It is shaded in dark grey the percentages upper than 50% and in light grey the percentages between 30 and 50%.

Index	January		February		March		April		May		June		July		August		September		October		November		December	
	+	–	+	–	+	–	+	–	+	–	+	–	+	–	+	–	+	–	+	–	+	–	+	–
TN10		17		8		33	3	6	17	6		46	3	6	8	6	6	6		67		50		25
TN90	6	8	6	8	14	3	3	3		3	6	8		3	3	6		8	3	3	67			11
TX10		11		8		39	3	3	19			42			3	3	3	3		22		17		6
TX90	8	3	8		22		19				8		3		53		25		36		56		3	22

low-level flow, is generally related to warm (cold) surface temperature anomalies in central Argentina, especially in winter (Barros *et al.*, 2002). Taking into account this impact on mean temperatures, the changes of the intensity of both the semi-permanent South Atlantic and Pacific anticyclones were analysed, as well as their potential relationship with the trends of the extreme temperature indices studied.

Figure 5 shows the decadal averages of sea level pressure at each month of the year. The dotted line shows the 1004 hPa isobar and solid line shows the 1018 hPa isobar, except for winter (June–September) when the 1020.5 hPa isobar was used because anticyclones are more intense at that time of the year. It is possible to see that from the 1971–1980 decade to the 2001–2010 decade the most significant shifts occur in the Atlantic, they are systematic and moving towards the West in June, August and October.

3.2.2. Relationship between the intensity of the South Atlantic anticyclone, the meridional flow (MF) and extreme temperature indices

In order to analyse the influence of the semi-permanent South Atlantic anticyclone and the MF over the region studied, two indices were developed.

The local intensity of the western flank of the mentioned anticyclone (AI) was measured by the mean geopotential height at 1000 hPa (G1000) in the Z1 region (Figure 3). This area has the major sea level pressure variability among the months during the studied period as it was observed in Figure 5.

The MF was analysed through the meridional wind at 925 hPa in the 28°–35°S, 57°–64°W region (Z3 in Figure 3). Significant negative correlations between both indices were found from March to October. This reflects that a more intense South Atlantic anticyclone is related to more intense winds from the north (or less intense winds from south) for the months mentioned. In fact, the northerly wind component is related with the geopotential gradient between the Chaco Low and the South Atlantic anticyclone, not just only the intensity of the anticyclone. Following Barros *et al*. (2002), we estimated a geopotential gradient at 925 hPa as the difference between geopotential height averaged from 25° to 35°S at 65° and 42.5°W, respectively. Significant high correlations throughout the year were found when MF at Z3 and the geopotential gradient were considered, with a mean determination coefficient (r^2) close to 0.6. Even though both Chaco low and South Atlantic anticyclone contribute to this gradient, the contribution of both systems is different throughout the year. In general terms, the contribution of Chaco low (Anticyclone) is stronger in summer (winter), and this was reflected in the relations mentioned earlier.

Especial attention was given to June and August, two of the months with the greatest shift of the South Atlantic anticyclone to the west among the different decades (Figure 5). Trends of AI were evaluated by means of the slope test, which resulted in significant positive trends at 10% in June and 5% in August. When the MF was

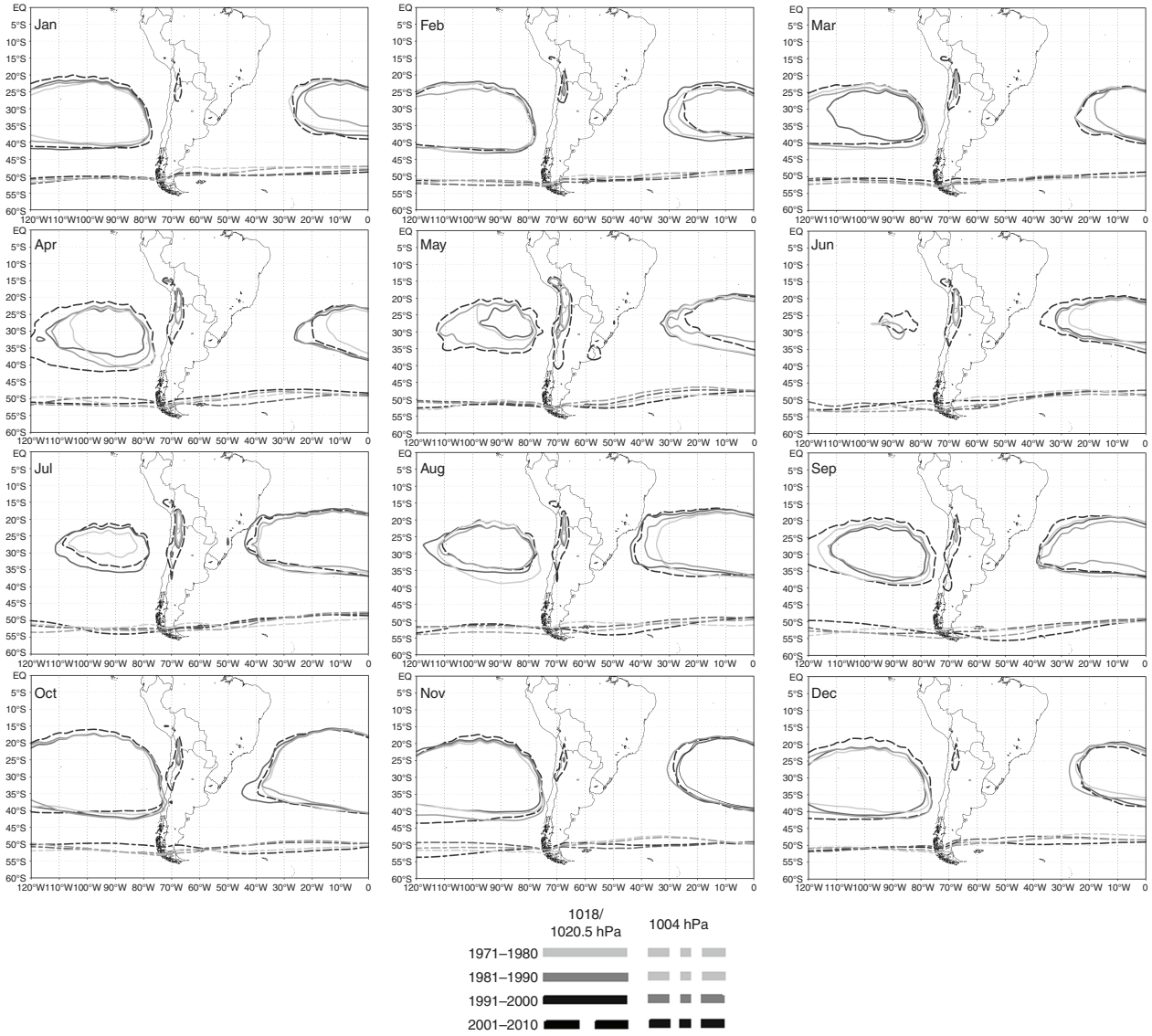

Figure 5. Decadal average of sea level pressure of NCEP/NCAR Reanalysis1 for each month of the year shown by selected contours: 1004 hPa and 1018 hPa (except for the winter months – June through September – in which the 1020.5 hPa isobar is shown).

analysed, a significant negative trend (7% level in August and 11% level at June) was found. This behaviour indicates an increase in the northern wind coinciding with a more intense South Atlantic anticyclone during the period 1970–2010 in June and August. It must be highlighted that these results only reflect a long-term behaviour of the indices, and they do not necessarily show an interannual co-variability.

In order to evaluate the relationship between the interannual variability of monthly temperature extremes and the intensity of the semi-permanent South Atlantic anticyclone, Spearman's correlation coefficient between AI and the extreme temperature indices for each station were performed. For this purpose, trends were filtered from all series, as explained in the previous section.

The TN90 extreme temperature index shows the highest number of months correlated with AI (Figure 6). The frequency of warm nights has significant positive correlations in a great number of stations in April and May and from July through November, especially in the central and south of the region studied. The positive correlation between both variables indicates that an increase (decrease) in TN90 is associated with an increase (decrease) in the 1000 hPa geopotential height in the Z1 region at interannual time scale.

Another index exhibiting several months with significant correlations is TN10, although in this case correlations are negative. The months of April, May, September and December show significant negative correlations towards the east of the region, and in October and November towards the central-south and southeast of the region studied, respectively. Besides, February tends to have an opposite behaviour as it presents some stations with positive correlations. The negative correlation between TN10 and the geopotential height indicates that a decrease (increase) in the occurrence of cold nights is associated with an increase (decrease) in the geopotential height in the Z1 region (Figure 7).

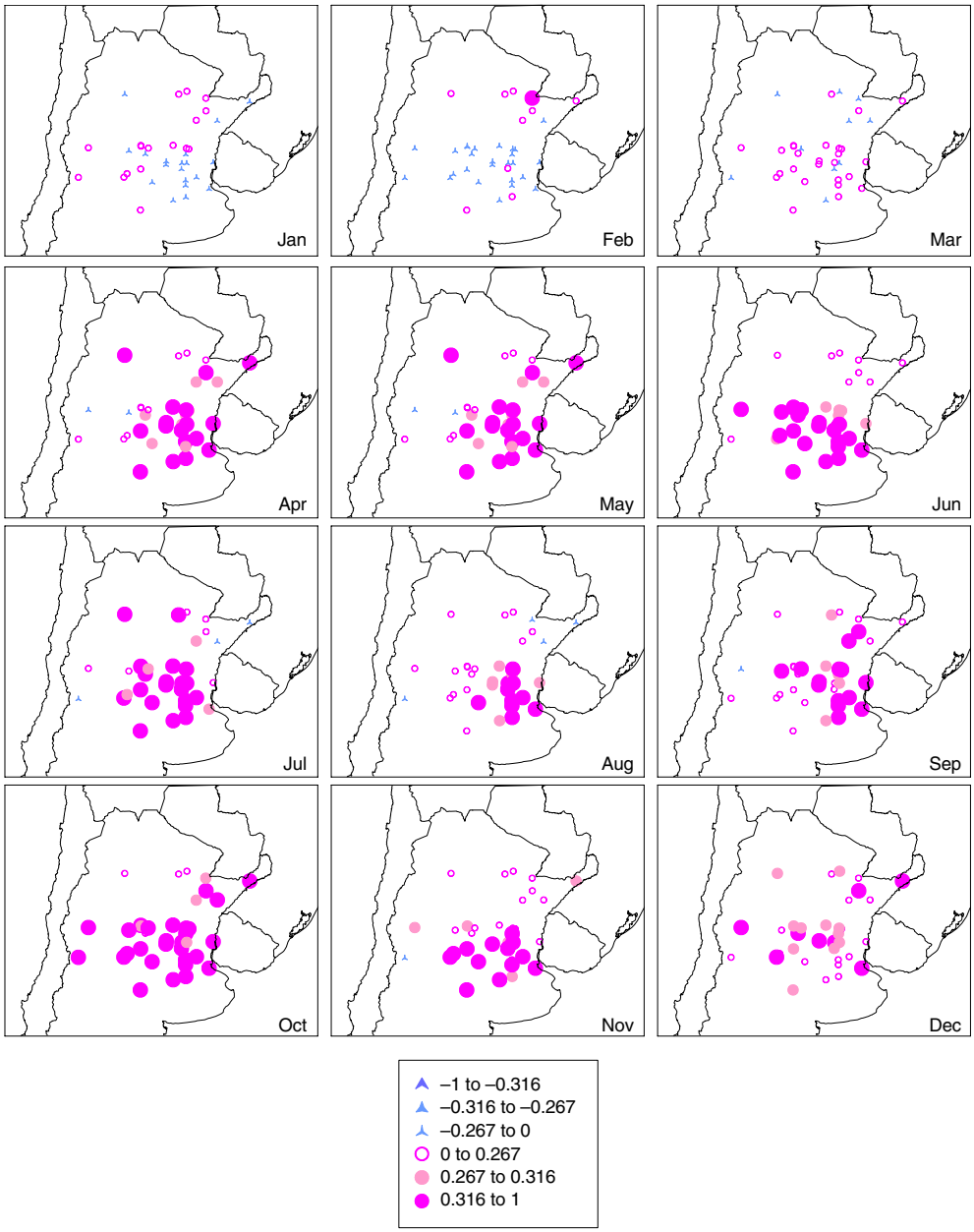

Figure 6. Correlation between the anomaly at 1000 hPa geopotential height with the TN90 index, where ▲ and ▲ indicate significant negative correlations at 5 and 10%, respectively, ● and ● indicate significant positive correlations at 5 and 10%, respectively, and ⅄ and ○ represent non-significant negative and positive correlations, respectively.

The maximum temperature indices show a lower relationship with AI. Significant correlations between the index of cold days and the geopotential height anomalies are scarce. Worth highlighting is the month of December, which shows significant negative correlations mainly in the eastern region. Lastly, the frequency of warm days is positively correlated with the geopotential height in May, August, October and November–the three latter only in the southeast of the region studied, in a significant way.

To conclude, the indices related to cold extremes (mainly TN10) generally show significant negative correlations with AI whereas those related to warm extremes show positive correlations. This can be better understood considering that AI is significantly correlated with the northern wind at Z3 during autumn, winter and spring, so warmer conditions are favoured when the South Atlantic anticyclone is more intense.

Furthermore, the results obtained were compared against the correlations obtained if the trend had not been filtered in order to see if the months highlighted in Section 3.2.1. had any difference in their correlations due to significant trends. Correlations between AI and the frequency of cold nights differ from the previous calculation only in the month of June, since it can be observed that there are a higher number of stations with significant correlations if trends are not previously filtered. In the case of cold days, it should be pointed out that due to the TX10 significant

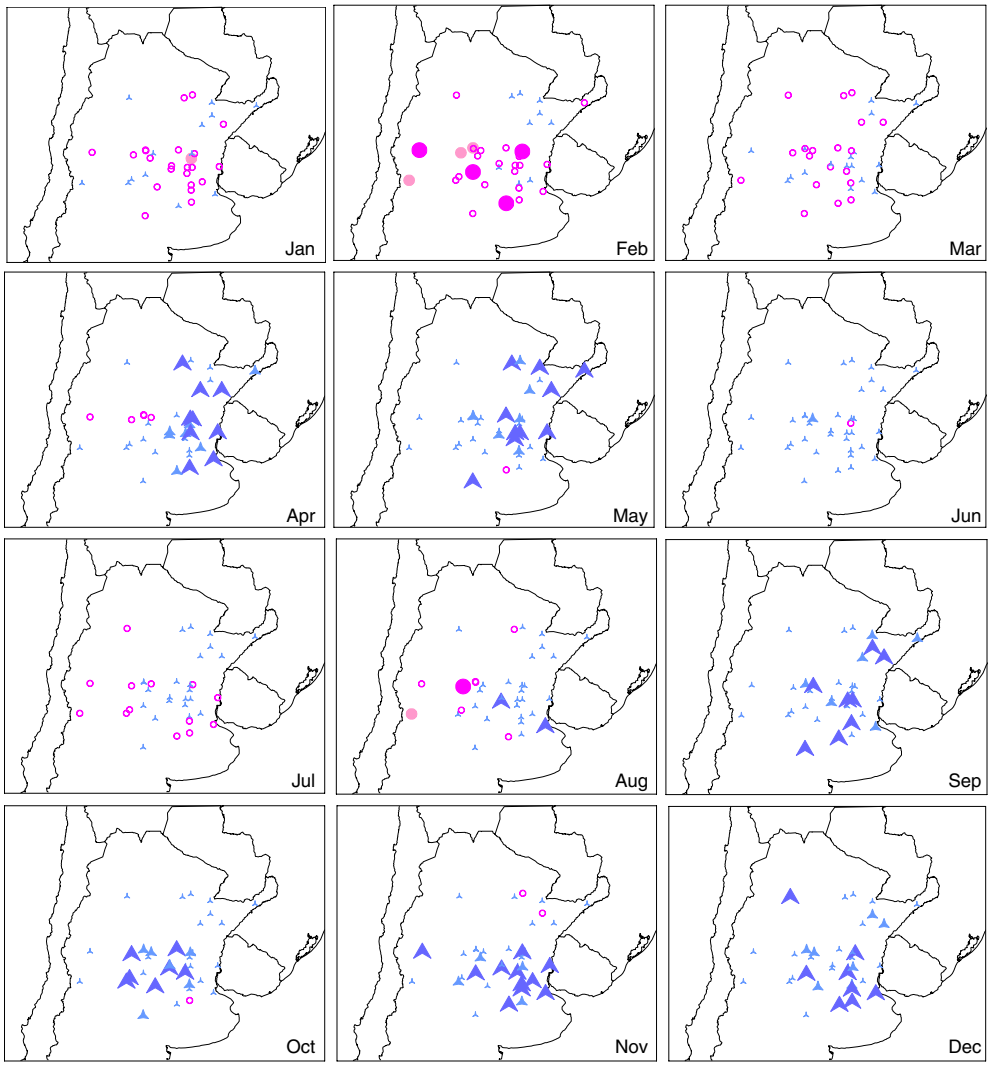

Figure 7. Same as Figure 6 for TN10.

negative trends and the positive trends of geopotential height in June, spurious significant negative correlations are obtained in the eastern part of the region studied if the series are not filtered. August also shows spurious significant positive correlations towards the west of the region studied when series are not filtered due to the significant positive trends of TX90 and geopotential height. It was concluded that June and August are associated in the long term with the intensity variability of the South Atlantic anticyclone, due to the fact that the extreme indices and G1000 in Z1 show significant trends in these months, and not at an interannual scale.

3.2.3. Relationship between the subtropical jet stream intensity and the indices of temperature extremes

According to Bejarán and Barros (2000), to the north of 40°S, the monthly mean cooling is the result of cold air breakouts towards the north and warming conditions in the region predominate when the frontal zone remains at higher latitudes. On the other hand, the shift of the fronts towards the north is associated with a similar change in the subtropical jet stream; i.e. the flow is intensified in the northern flank of the Westerlies belt and it gets weaker at mid-latitudes. The opposite takes place when the frontal zone remains at mid-latitudes.

Müller *et al.* (2005) analysed the mean atmospheric circulation associated with generalized frost in central southern South America. They found an intensification (weakening) of the subtropical jet over South America in the case of frosts above (below) average in the region analysed, in the monthly and seasonal composites. Moreover, they suggested that the intensification of the jet might be related to an amplification of the pressure gradient in the region due to the increase in Rossby wave activity. Finally, they claimed that the weakening of the subtropical jet around 25°S favours the occurrence of positive temperature anomalies as this allows a quick passage of frontal systems to the north of 30°S and the re-establishment of the circulation with a northern component over most of Argentina.

To identify the relationship between the position of subtropical jet and extreme temperature occurrence, the Spearman's correlation coefficient was calculated between the zonal wind at 250 hPa in the Z2 region and the temperature

extreme indices. Before correlations were calculated, the monthly trends of the zonal wind at 250 hPa (u250) were analysed, and no significant trends at 10% were found.

Significant positive correlations were found between u250 and cold indices (TN10 and TX10), whereas negative correlations were found in warm indices (TN90 and TX90). Positive correlations indicate that a decrease (increase) in the intensity of the zonal wind at 250 hPa is associated with a reduction (increase) in the frequency of cold extremes; this result is consistent with the findings reached by Bejarán and Barros (2000) regarding the monthly mean temperature. u250 gets stronger between 25° and 35°S, due to the northward movement of the frontal systems that fosters surface cooling. If the zonal wind intensifies at mid-latitudes, the cold fronts will not keep moving northward, spurring warmer conditions at the weather stations analysed in this study. Therefore, it is also coherent for the correlation between the zonal wind and the warm indices to be negative.

The frequency of warm days shows significant negative correlations with u250 in all months in most of the weather stations analysed, except for July, while November only shows significant correlations in the east of the region studied. Throughout the year, the TX90 index shows the highest number of months with significant correlations with the u250 (Figure 8) in several stations.

3.2.4. Influence of ENSO on temperature extremes

ENSO is the greatest variability mode in the tropical Pacific and is responsible for most interannual variability affecting the climate all over the world. Even considering the differences between diverse El Niño or La Niña events (not all events produce the same impact), the literature shows in general terms warmer (cooler) conditions under El Niño (La Niña) phases during winter (autumn and winter) over central Argentina. These characteristics reflect mean conditions and they cannot be extrapolated directly to extreme temperature conditions. In a great part of Central Argentina, for example, very little association exists between mean seasonal temperature and the occurrence of warm or cold days during winter (Rusticucci and Barrucand, 2004).

In order to analyse the impact of ENSO phases on temperature extreme frequency throughout the year, differences between the frequency distributions of temperature extremes (considering all stations as a whole) associated with each ENSO phase and climatology were tested at a 5% significant level using the methodology mentioned in Section 2. Results are presented at Table 2 (El Niño *vs* climatology) and Table 3 (La Niña *vs* climatology) for the four indices of extreme temperature. The signs indicate a significant higher (+) or lower (−) frequency of temperature extremes during the phase mentioned with respect to the climatologic expected frequency.

During El Niño years, fewer warm days and more cold days are expected during late spring (in the case of warm days) and summer months. With respect to warm and cold nights, differences are not as clear during this season, except for December, when warmer conditions are observed. During winter months (May–September), the strongest signal can be seen in minimum extremes, resulting in more frequent warmer nights and less frequent cold nights.

Almost the opposite occurs during La Niña. Table 3 shows that since November to February, almost all months present more (fewer) frequent warm days (cold days) than the climatology. In the same way, Arblaster and Alexander (2012) showed that, the extreme 1-day annual maximum temperature is almost 1 or 2 °C higher during La Niña years than El Niño in DJF in our region analysing 1950–1999 events.

December clearly shows high diurnal range during La Niña, just the opposite to what was observed during El Niño. On winter months, cooling conditions are favoured under La Niña phase. This is reflected especially in July and August, with more frequent cold nights and days.

If we compare the results presented at Table 2 with respect to those found by Kenyon and Hegerl (2008) over central Argentina, it is possible to see the agreement in relation to warm extremes temperatures results: more warm nights but fewer warm days during the extended warm season (November–April) are observed under El Niño phase. However, when cold nights are analysed, the authors found less cold nights and higher extreme minimum temperatures for the same period, concurring with warmer conditions. Nevertheless, a more detailed analysis over a monthly basis and reflected here on Table 2 shows that the effect over the cold extremes TN10 is not uniform along all the period November–April, and it is possible to clearly observe the intra-annual difference in the responses.

To conclude, it is possible to see that ENSO's phases have an impact on the probability of temperature extremes, fostering or hampering their development. Previous studies showed that the region considered had a predominance of warmer mean temperature conditions during El Niño in the winter months, while in summer, no significant relationship could be seen. These results are consistent with the findings of this work, which analyses each temperature extreme separately. In the winter months, both the minimum and the maximum temperature extremes show a tendency towards warmer conditions. By late spring and early summer, however, only the minimum temperature extremes show this feature, while the maximum temperature extremes behave contrariwise. This is the reason why previous studies could not find a significant relationship between ENSO's phases and the mean temperature in the region surveyed. Considering the effect on both temperature extremes, it is possible to conclude that El Niño fosters a temperature range decrease in the region during summer and a warming during winter, i.e there is less intra-annual variability during warm ENSO phase in the region.

4. Summary and conclusions

The aim of this study is to analyse the interannual variability of monthly climatic indices of extreme daily

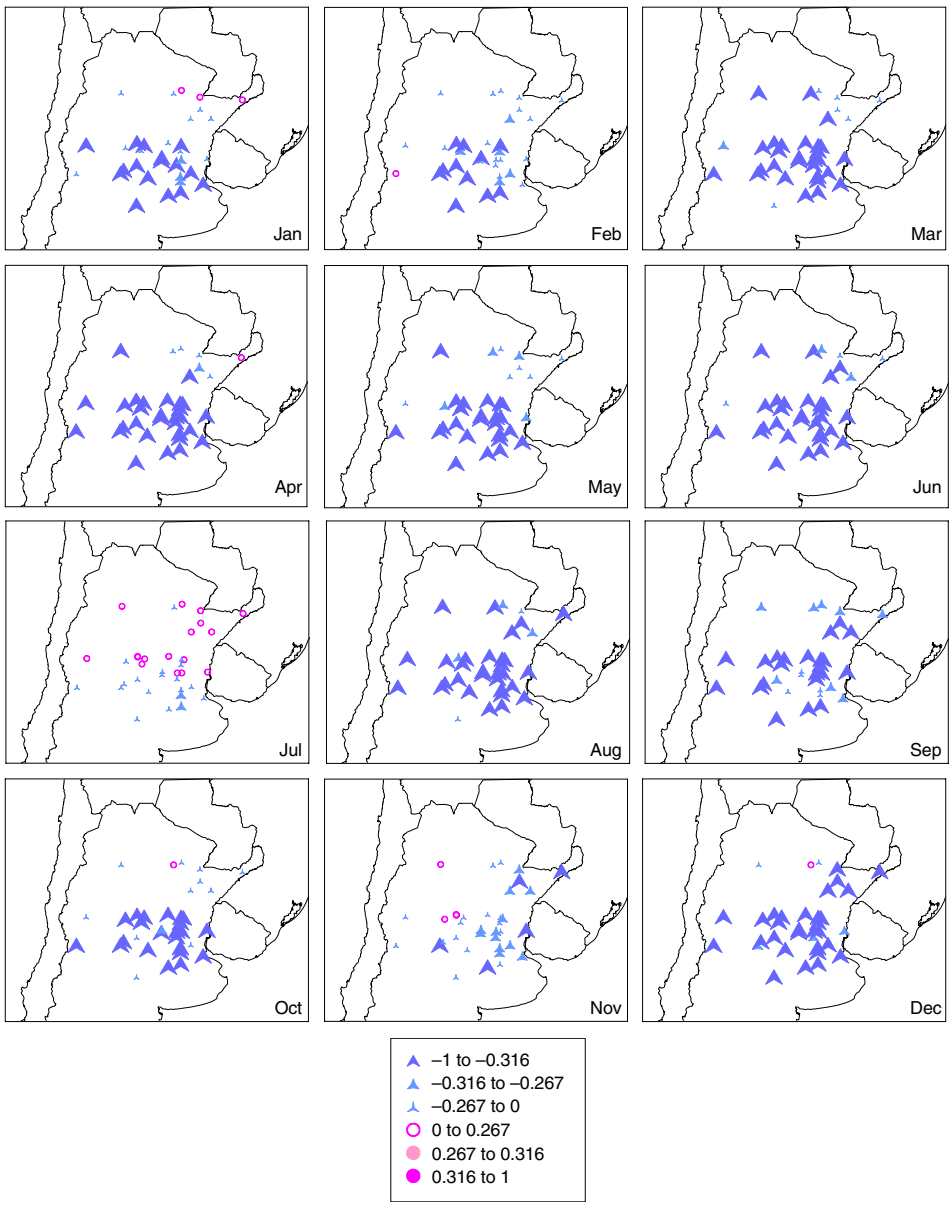

Figure 8. Correlation between the zonal wind in 250 hPa with the TX90 index, where ▲ and ▲ indicate significant negative correlations at 5 and 10%, respectively, ● and ● indicate significant positive correlations at 5 and 10%, respectively, and ⅄ and ○ represent non-significant negative and positive correlations, respectively.

Table 2. Significant differences at 5% (Wilcoxon test) between the frequency distribution of El Niño and climatology events for the four indices of extreme temperature. Signs indicate a higher or lower (+/−) occurrence of temperature extremes during this phase. It is shaded in dark (light) grey the months with cooler (warmer) conditions under El Niño phase with respect to the climatology.

	January	February	March	April	May	June	July	August	September	October	November	December
TN10		+			−		−		−			−
TN90		+	+	−	+	+	+	+	+			+
TX10	+	+		−	−	+		+	−			+
TX90	−	−		−	−	−	+	+	+		−	−

temperature in the central-north region of Argentina throughout a year and its relationship with the atmospheric circulation. The impact of both ENSO phases over different temperature extreme indices throughout the year is specially analysed.

The study on monthly trends of series of temperature extremes in the 1970–2010 period showed a significant decrease in the frequency of cold nights in October and November, a significant decrease in the frequency of cold days in March, June and October, and a significant increase in the occurrence of warm days in March, August, October and November. This means that it was possible to observe a decrease in the frequency of cold extremes and an increase in the occurrence of warm extremes that encourage warmer

Table 3. Same as Table 2 except for La Niña.

	January	February	March	April	May	June	July	August	September	October	November	December
TN10			+	+			+	+	−		+	+
TN90			−		−			−		−	−	−
TX10		−			+		+	+	−			−
TX90	+	+	−	+						−	+	+

conditions in the region studied. This was tested using a parametric methodology and a nonparametric one, yielding coinciding results.

Then, the variability of large-scale circulation was studied by analysing the changes in the position of the semi-permanent anticyclones of the Southern Hemisphere. The results showed a systematic and significant shift towards the west of the South Atlantic anticyclone over decades in the months of June and August, together with an increase in the north component of the wind in the region studied, measured by the meridional wind at 925 hPa in central Argentina, which could account for the decrease in cold nights and days in June in the long term and the increase in warm days in August.

Subsequently, in order to evaluate the interannual co-variability, correlations between extreme temperature indices and series of monthly mean anomalies of geopotential height at 1000 hPa in the region with the greatest shift towards the west of the Atlantic anticyclone were calculated. The findings showed significant negative correlations with the TN10 index, mainly in spring and in April and May, while positive correlations were found with warm extremes, except for summer, where no significant correlations were found. Therefore, at an interannual scale, the intensification of the western part of the anticyclone, which fosters warm air advection from the north, coincides with a greater frequency of warm extremes and with a lower frequency of cold extremes.

Analyses were also made on the variations of the intensity of the subtropical jet stream that affects the latitudinal progress of cold air associated with the passage of frontal systems. It was possible to find significant positive (negative) correlations between the intensity of the jet and cold (warm) indices in several months. The zonal component of the wind at 250 hPa between 25° and 35°S intensifies when cold fronts move towards the north. If this movement is not so marked towards the north and the fronts remain at mid-latitudes, then the zonal wind at 250 hPa is weaker. This intensification fosters the occurrence of extreme cold events.

Finally, the impact of ENSO phases on temperature extreme frequency throughout the year was analysed. Differences between the frequency distributions of temperature extremes in central Argentina associated with each ENSO phase and climatology were tested at a 5% significant level using the nonparametric Wilcoxon rank-sum test.

These results show that the impact of the El Niño event on extreme temperatures in the region has differences by month, fostering a warming during winter (more warm nights and days are observed) and cooling condition in summer (less warm days and more cold days are observed). December (principally) and January are characterized by a decrease in the diurnal temperature range.

This decrease in the diurnal and annual range could be due to the increase in precipitation, associated with more advection of humid air from the north, related to the position of the subtropical jet mentioned.

Almost the opposite occurs during La Niña. Since November–February, almost all months present more (fewer) frequent warm days (cold days) than the climatology. December exhibits a high diurnal range and winter months are affected by cooling conditions (more cold days and nights, especially in July and August).

This more detailed study presents the intra-annual variability responses of extreme temperatures to changes of the main relevant circulation features affecting the central area of Argentina, both the most populated and productive. The results identifying the impact of ENSO phases, the position of subtropical and LLJs, will aid in defining predictors of extreme events on monthly and seasonal scales.

Acknowledgements

This research has been funded by 20020130100263BA and 20020130200142BA from the University of Buenos Aires and CONICET PIP0227 projects. The authors wish to thank the two anonymous reviewers for their very useful comments that improved this article.

Supporting information

The following supporting information is available as part of the online article:

Figure S1. Decadal average of geopotential height at 1000 hPa of NCEP/NCAR Reanalysis1, NCEP/DOE R2, ERA-Interim, 20CR v2c and JRA-55 for each month of the year shown by two selected contours: 155 m (dotted lines) and −20 m (solid line). Except for the winter months (June through September) in which the 175 m height contour is shown on a solid line.

Figure S2. Correlation between the anomaly at 1000 hPa geopotential height with the TN10 index in the 1971–2010 period for three different reanalysis: NCEP/NCAR Reanalysis1, 20CR v2c and JRA-55, where ● and ● indicate significant negative correlations at 5 and 10%, respectively, ● and ● indicate significant positive correlations at 5 and 10%, respectively, and ○ and ○ represent

non-significant negative and positive correlations, respectively.

Figure S3. Same as Figure S2 for TN90 index.

Figure S4. Same as Figure S2 for TX10 index.

Figure S5. Same as Figure S2 for TX90 index.

Figure S6. Correlation between the anomaly at 1000 hPa geopotential height with the TN10 index in the 1979–2010 period for five different reanalysis: NCEP/NCAR Reanalysis1, NCEP-DOE Reanalysis2, ERA-Interim, 20CR v2c and JRA-55, where ● and ● indicate significant negative correlations at 5 and 10%, respectively, ● and ● indicate significant positive correlations at 5 and 10%, respectively, and ○ and ○ represent non-significant negative and positive correlations, respectively.

Figure S7. Same as Figure S6 for TN90 index.

Figure S8. Same as Figure S6 for TX10 index.

Figure S9. Same as Figure S6 for TX90 index.

Figure S10. Correlation between zonal wind at 250 hPa with the TN10 index in the 1971–2010 period for three different reanalysis: NCEP/NCAR Reanalysis1, 20CR v2c and JRA-55, where ● and ● indicate significant negative correlations at 5 and 10%, respectively, ● and ● indicate significant positive correlations at 5 and 10%, respectively, and ○ and ○ represent non-significant negative and positive correlations, respectively.

Figure S11. Same as Figure S10 for TN90 index.

Figure S12. Same as Figure S10 for TX10 index.

Figure S13. Same as Figure S10 for TX90 index.

Figure S14. Correlation between zonal wind at 250 hPa in Z2 region with the TN10 index in the 1979–2010 period for five different reanalysis: NCEP/NCAR Reanalysis1, NCEP-DOE Reanalysis2, ERA-Interim, 20CR v2c and JRA-55, where ● and ● indicate significant negative correlations at 5 and 10%, respectively, ● and ● indicate significant positive correlations at 5 and 10%, respectively, and ○ and ○ represent non-significant negative and positive correlations, respectively.

Figure S15. Same as Figure S14 for TN90 index.

Figure S16. Same as Figure S14 for TX10 index.

Figure S17. Same as Figure S14 for TX90 index.

References

Agosta E, Barrucand M. 2012. Condiciones medias de invierno y ondas cuasi-estacionarias de Rossby asociadas a la frecuencia invernal de noches frías y cálidas en Argentina Subtropical. *Geoacta* **37**(2): 147–166, ISSN 1852-7744.

Alexander LV, Zhang X, Peterson TC, Caesar J, Gleason B, Klein Tank AMG, Haylock M, Collins D, Trewin B, Rahimzadeh F, Tagipour A, Rupa Kumar K, Revadekar J, Griffiths G, Vincent L, Stephenson DB, Burn J, Aguilar E, Brunet M, Taylor M, New M, Zhai P, Rusticucci M, Vazquez-Aguire JL. 2006. Global observed changes in daily climate extremes of temperature and precipitation. *J. Geophys. Res.* **111**: D05109, doi: 10.1029/2005JD006290.

Arblaster JM, Alexander LV. 2012. The impact of the El Niño-Southern Oscillation on maximum temperature extremes. *Geophys. Res. Lett.* **39**: L20702, doi: 10.1029/2012GL053409.

Arnau Gras J. 2001. Diseños de series temporalis: técnicas de análisis. Colección de la Universidad de Barcelona (UB 46). Edicions de la Universitat de Barcelona, 434 pp.

Barros V, Grimm A, Doyle M. 2002. Relationship between temperature and circulation in southeastern South America and its influence from El Niño and La Niña events. *Journal of the Meteorological Society of Japan* **80**(1): 21–32.

Barrucand M. 2008. *Extremos de temperatura en Argentina: cambios observados en la variabilidad espacio-temporal y su relación con otras características del sistema climático*. Tesis doctoral, Universidad de Buenos Aires.

Barrucand M, Rusticucci M. 2001. Climatología de temperaturas extremas en la Argentina. Variabilidad temporal y regional. *Meteorologica* **26**: 85–101.

Bejarán R, Barros V. 2000. Influence of some atmospheric circulation indices on the mean monthly temperature in central and northern Argentina.11° Brazilian Congress of Meteorology, SBMET CD-ROM CL 00104.5 pp (in Spanish).

Freund JE, Miller I, Miller M. 2000. *Estadística matemática con aplicaciones*. Sexta edición edn. Pearson Educación: Naucalpán de Juarez, Mexico, 640 pp.

Garreaud R. 2009. The Andes climate and weather. *Adv. Geosci.* **22**: 3–11.

Garreaud R, Vuille M, Compagnucci R, Marengo J. 2009. Present-day South American climate. *Palaeogeogr. Palaeoclimatol. Palaeoecol.* **281**(3–4): 180–195, doi: 10.1016/j.palaeo.2007.10.032.

Gibbons JD, Chakraborti S. 2011. *Nonparametric Statistical Inference*, 5th edn. Chapman & Hall/CRC Press, Taylor & Francis Group: Boca Raton, FL.

Gosling S, Dunn R, Carrol F, Christidis N, Fullwood J, de Gusmao D, Golding N, Good L, Hall T, Kendon L, Kennedy J, Lewis K, McCarthy R, McSweeney C, Morice C, Parker D, Perry M, Stott P, Willett K, Allen M, Arnell N, Bernie D, Betts R, Bowerman N, Brak B, Caesar J, Challinor A, Dankers R, Hewer F, Huntingford C, Jenkins A, Klingaman N, Lowe J, Lloyd-Hughes B, Miller J, Nicholls R, Noguer M, Otto F, van der Linden P, Warren R. 2011. *Climate: observations, projections and impacts*. Met Office. Available at http://www.metoffice.gov.uk/media/pdf/1/l/Argentina.pdf (accessed 15 March 2016).

Grimm AM, Barros VR, Doyle M. 2000. Climate variability in southern South America associated with El Niño and La Niña events. *J. Clim.* **13**: 35–58.

Hartmann DL, Klein Tank AMG, Rusticucci M, Alexander LV, Brönnimann S, Charabi Y, Dentener FJ, Dlugokencky EJ, Easterling DR, Kaplan A, Soden BJ, Thorne PW, Wild M, Zhai PM. 2013. Observations: atmosphere and surface. In *Climate Change 2013: The Physical Science Basis. Contribution of Working Group I to the Fifth Assessment Report of the Intergovernmental Panel on Climate Change*, Stocker TF, Qin D, Plattner GK, Tignor M, Allen SK, Boschung J, Nauels A, Xia Y, Bex V, Midgley V (eds). Cambridge University Press: Cambridge, UK and New York, NY.

Haylock MR, Peterson TC, Alves LM, Ambrizzi T, Anunciaçao T, Baez J, Barros VR, Berlato MA, Bidegain M, Coronel G, Corradi V, Garcia VJ, Grimm AM, Karoly D, Marengo JA, Marino MB, Moncunill DF, Nechet D, Quintana J, Rebello E, Rusticucci M, Santos JL, Trebjo I, Vincent LA. 2006. Trends in total and extreme South American rainfall in 1960–2000 and links with sea surface temperature. *J. Clim.* **19**: 1490–1511, doi: 10.1175/JCLI3695.1.

Hoel P. 1971. *Introduction to Mathematical Statistics*. Wiley and Sons Inc.: New York, NY, 409 pp.

Houghton JT, Ding Y, Griggs DJ, Noguer M, van der Linden PJ, Dai X, Maskell K, Johnson CA. 2001. *Climate Change 2001: The Scientific Basis*. Contribution of Working Group I to the Third Assessment Report of the Intergovernmental Panel on Climate Change. Cambridge University Press: Cambridge, UK and New York, NY, 881 pp.

IPCC. 2012. Managing the risks of extreme events and disasters to advance climate change adaptation. In *A Special Report of Working Groups I and II of the Intergovernmental Panel on Climate Change*, Field CB, Barros V, Stocker TF, Qin D, Dokken DJ, Ebi KL, Mastrandrea MD, Mach KJ, Plattner GK, Allen SK, Tignor M, Midgley PM (eds). Cambridge University Press: Cambridge, UK, 582 pp.

Karoly DJ. 1989. Southern Hemisphere circulation features associated with El Niño–Southern Oscillation events. *J. Clim.* **2**: 1239–1252.

Kenyon J, Hegerl GC. 2008. Influence of modes of climate variability on global temperature extremes. *J. Clim.* **21**: 3872–3889, doi: 10.1175/2008JCLI2125.1.

Marengo J, Soares C, Saulo C, Nicolini M. 2004. Climatology of the LLJ east of the Andes as derived from the NCEP reanalyses. *J. Clim.* **17**: 2261–2280.

Mo K. 2000. Relationships between low-frequency variability in the Southern Hemisphere and sea surface temperature anomalies. *J. Clim.* **13**: 3599–3620.

Müller GV, Ambrizzi T, Nuñez MN. 2005. Mean atmospheric circulation leading to generalized frosts in central southern South America. *Theor. Appl. Climatol.* **82**: 95–112, doi: 10.1007/s00704-004-0107-y.

Nakamura H, Sampe T, Tanimoto Y, Shimpo A. 2004. Observed associations among storm tracks, jet streams and midlatitude oceanic fronts. In *Earth's Climate*, Wang C, Xie SP, Carton JA (eds). American Geophysical Union: Washington, DC, doi: 10.1029/147GM18.

Prohaska FJ. 1976. *Climates of Central and South America. World Survey of Climatology*. Elsevier: Amsterdam, vol. 12, 532 pp.

Rusticucci M. 2012. Observed and simulated variability of extreme temperature events over South America. *Atmos. Res.* **106**: 1–17.

Rusticucci M, Barrucand M. 2001. Climatología de temperaturas extremas en la Argentina. Consistencia de datos. Relación entre la temperatura media estacional y la ocurrencia de días extremos. *Meteorológica* **26**: 69–83.

Rusticucci M, Barrucand M. 2004. Observed trends and changes in temperature extremes over Argentina. *J. Clim.* **17**: 4099–4107, doi: 10.1175/1520-0442(2004)017<4099:OTACIT>2.0.CO;2.

Rusticucci M, Vargas W. 2002. Cold and warm events over Argentina and their relationship with the ENSO phases: risk evaluation analysis. *Int. J. Climatol.* **22**: 467–483.

Saulo AC, Nicolini M, Chou SC. 2000. Model characterization of the South American low-level flow during the 1997–98 spring-summer season. *Clim. Dyn.* **16**: 867–881.

Seluchi M, Saulo C. 2012. Baixa do Noroeste Argentino e Baixa do Chaco: caracterísitcas, diferenças e semelhanças (the northewestern Argentinean low and the Chaco Low: their characteristics, differences and similarities). *Rev. Bras. Meteorol.* **27**(1): 49–60.

Sen PK. 1968. Estimates of the regression coefficient based on Kendall's tau. *J. Am. Stat. Assoc.* **63**: 1379–1389.

Skansi M, Brunet M, Sigró J, Aguilar E, Arevalo Groening JA, Bentancur OJ, Castellón Geier YR, Correa Amaya RL, Jácome H, Malheiros Ramos A, Oria Rojas C, Pasten AM, Sallons Mitro S, Villaroel Jiménez C, Martínez R, Alexander LV, Jones PD. 2013. Warming and wetting signals emerging from analysis of changes in climate extreme indices over South America. *Global Planet. Change* **100**: 295–307.

Tencer B, Rusticucci M. 2012. Analysis of interdecadal variability of temperature extreme events in Argentina applying EVT. *Atmósfera* **25**(4): 327–337.

Vera C, Silvestri G, Barros V, Carril A. 2004. Differences in El Niño response over the Southern Hemisphere. *J. Clim.* **17**: 1741–1753.

Vincent LA, Peterson TC, Barros VR, Marino MB, Rusticucci M, Carrasco G, Ramirez E, Alves LM, Ambrizzi T, Berlato MA, Grimm AM, Marengo JA, Molion L, Moncunill DF, Rebello E, Anunciação YMT, Quintana J, Santos JL, Baez J, Coronel G, Garcia J, Trebejo I, Bidegain M, Haylock MR, Karoly D. 2005. Observed trends in indices of daily temperature extremes in South America 1960–2000. *J. Clim.* **18**: 5011–5023, doi: 10.1175/JCLI3589.1.

Wilcoxon F. 1945. Individual comparisons by ranking methods. *Biometrics* **1**: 80–83.

Wilks DF. 2006. *Statistical Methods in the Atmospheric Sciences*, 2nd edn. Academic Press: USA, 627 pp.

